Jurnal Mekanikal
December 2007, No. 24, 15 - 31

CRUSHING BEHAVIOR OF PULTRUDED COMPOSITES

Al Emran Ismail[*], Afizun Ahmad

Faculty of Mechanical & Manufacturing Engineering,
Universiti Tun Hussin Onn Malaysia (UTHM),
Parit Raja, Batu Pahat, 86400 Johor

ABSTRACT

An experimental investigation was carried out to study the crashworthiness parameters and behavior of pultruded composite tubes. Quasi-static compressive loadings were applied axially on pultruded composite to investigate the response of force-displacement during progressive collapses. Three chamfering angles 35°, 45° and 55° were selected to study their effect on crushing behaviors and collapse modes. Load-displacement curves and collapse mode of each sample is presented and discussed. The results showed that higher chamfering angle produced higher energy absorption capability. Progressive collapses are 5 mm thick wall composites, while for 3 mm thick wall composites, global buckling occurred on the wall sides after fast unstable crack propagation along the tube corners.

Keywords: *Pultruded composites, crashworthiness, energy absorption, collapse mod, progressive collapse.*

1.0 INTRODUCTION

Safety is one of the most urgent issues among various requirements in vehicles such as cars, helicopters, trains, etc., because protecting passengers from accidental collisions is a daily need. The car body for example, should possess high performance in protecting passengers, i.e. a high energy-absorption capability, and many different systems have been proposed in designing the body and its components. Regarding scientific research in this field, a technological term Crashworthiness is often used and a special international conference and a journal on crashworthiness have appeared. These movements must lead to the development of effective crush elements in various vehicles [1].

One of the current design theories for passenger vehicles is to have a progressively compliant front end [2] and a rigid passenger compartment. A progressively complaint front end consists of a series of crumple zones, each resisting deflection until a certain load level is reached and then deforming at that constant load level until the next zone is reached. The first zone deforms at a very low load level to protect pedestrians and cyclists. The series of zones that follow are designed for increasing levels of loads; the final zone is the rigid passenger compartment which should resist all deflection.

---

[*] Corresponding author: E-mail: emran@uthm.edu.my

Most of the research on the energy absorption of metals has concentrated on thin walled cylinders of simple cross section and fairly well understood. Most fiber reinforced composites absorb energy through a combination of fracture and friction [3], whereas metals absorb energy through plastic deformation [4, 5]. In order for either a metal or a composite to absorb energy efficiently, stable progressive crushing must occur. A stable progressive crush is characterized by localized failure that begins at one end of the specimen and progresses through the specimen without significantly damage past this crush front. To ensure stable crushing in both metals and fiber reinforced composites a crush initiator which creates a local stress concentration is used. If stable crushing is not established the specimen will then usually fail catastrophically. During catastrophic failure the peak load is very high and drops off quickly so the average load is low. Catastrophic failures are clearly not acceptable for energy management.

The most common type of crush initiator used has been an external bevel or chamfer ground into one end of the specimen. Farley and Jones [6] showed that the corners of their specimens absorbed more energy than the flatter sections so that as the percentage of corners in the tube was increased so was the energy absorption. It has also been shown that the use and style of crush initiation affect the sustained crushing of materials [7]. The main objectives of this present investigation are to determine the load versus displacement response, energy absorption capability and collapse modes of as-received pultruded composite tubes. Different chamfering angles are introduced in the front ends to create a crush initiator and to study the effect of these angles on crashworthiness behaviors on pultruded composites.

2.0 METHODOLOGY

2.1 Material

As-received pultruded composites are delivered in 50 x 50 mm square tubes (3 and 5 mm thickness) with 1 m length for each material condition. Table 1 shows the elastic properties of chopped strand mat glass fiber used in this work. The fiber architecture of the pultruded tube consists of glass fiber roving at a 64% volume fraction in average. Fiber volume fraction depends on the composite length, where some fibers break during pultrusion process therefore, this fraction is not constant. Burning test is then conducted to remove polyester resin according to ASTM D2584 in furnace environment at temperature 55°C. Table 2 lists the results from this test.

Table 1: Elastic properties of chopped strand mat [8]

E_x (GPa)	E_y (GPa)	E_z (GPa)	G_{xy} (GPa)	G_{yz} (GPa)	G_{zx} (GPa)	υ_{xy}	υ_{yy}	υ_{zx}	ρ (kgm^{-3})
6.28	6.28	6.28	2.35	2.35	2.35	0.35	0.35	0.35	1494

Table 2: Burning test of pultruded composite

Specimen	W_f(g)	W_m(g)	W_f(%)	W_m(%)	ρ_c(kgm^{-3})	V_f(%)	V_m(%)
1	4.766	2.656	0.642	0.358	2.068	0.620	0.380
2	6.182	3.128	0.664	0.336	2.072	0.643	0.357
3	3.766	2.241	0.627	0.373	2.065	0.605	0.395
Average	4.904	2.675	0.6443	0.355	2.068	0.622	0.377

Front end of the tubes are chamfered at different angles such as 35°, 45° and 55°. These angles are machined using dry grinding machine in order to have identical angles. Low feeding rate is used during machining to reduce any residual stress and cracking. The total height for each sample is 100 mm.

2.2 Tensile Test

The rectangular composite test specimens with dimensions of 254 × 12.7 × 3.175 mm were cut from pultruded panels with a high speed cutter and edges were polished with very fine aluminum oxide sandpaper to remove heat affected zone or layer. Tensile testing of pultruded fiber glass composites specimens was performed using a GOTECH machine. Each specimen was tested to failure following the procedure in accordance with ASTM D3039-97. Constant cross-head displacement 1.5 mm/min is used to simulate quasi-static tensile loading imposed to pultruded composite. Figure 1 shows the dimension and configuration of sample for tensile test. Strain gauge is installed parallel to the loading direction. Then, stress versus strain curve is constructed and analyzed.

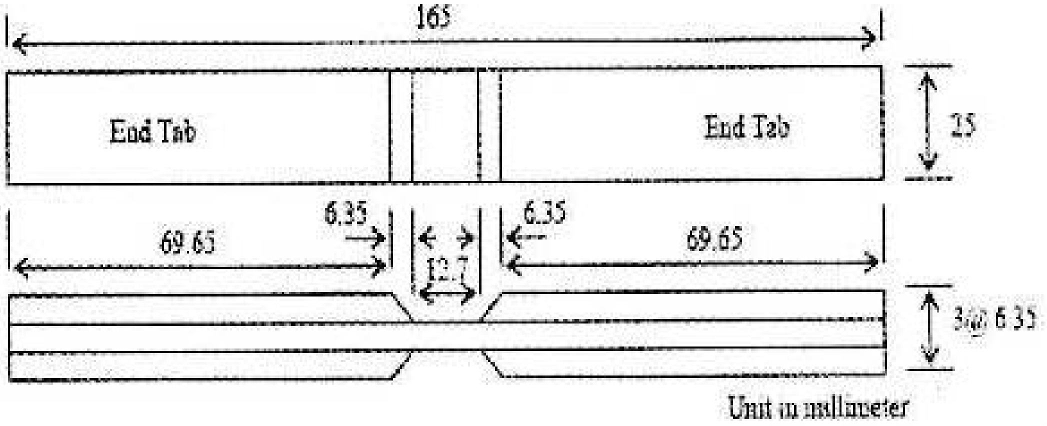

Figure 1: Tensile test set-up in this work [1]

2.3 Compressive Test

Quasi-static compression testing is conducted using GOTECH machine with a maximum load 100 kN and cross-head displacement of 1.5 mm/min. The composites are axially crushed between two parallel steel flat platens, one moving and one static. The sample and flat platen are properly aligned to prevent bending moment occurs during crushing process. For each test, the crush force is plotted against displacement on the Y-axis and X-axis, respectively. Progressive collapse for each sample is recorded and analyzed.

2.4 Crashworthiness Parameters

After the completion of the tests, crashworthiness parameters such energy absorption performances, mean compressive force and load ratio are extracted from force versus displacement response for each material conditions. These parameters are very crucial to consider the application of this material in crushing process.

2.4.1 Energy Absorption Capability

The values of the energy absorption capability were calculated from the force-displacement curves by smoothing out the force serrations to obtain mean forces of the load during each stage of crushing processes. Energy absorption capability during the structural crash is a requirement for the complete spectrum of passenger transportation. The total work done during the axial crushing of the pultruded composites is equal to the area under the force-displacement curves and is evaluated as in equation (1).

$$\text{Energy absorption, } E = \int P_i ds \tag{1}$$

Where P_i is an applied force and ds is displacement distance. Equation (1) can be simplified by averaging the serration forces during crushing process and mean force of the serration forces are then introduced and multiplied by crushed deformation displacement. The multiplication of mean force and crushed distance represent the energy absorbed by the composites or the area under the curve.

3.0 RESULTS AND DISCUSSION

3.1 Tensile Test

Figure 2 shows the average stress-strain diagram of as-received pultruded composite for both 5 mm and 3 mm under this investigation. The material shows linear elastic behavior until the final failure meaning that the material fails in brittle mode. At the final failure of Figure 2, push-pull phenomenon of fiber embedded in polymeric resin dominated to constrain from sudden failure. It is important to note that fibers effectively play its role in toughening the composite through effective shear force transfer. It is estimated that modulus of elasticity of this composite is about 5.7 GPa.

3.2 Load-Displacement Curves

In order to evaluate the crushing process of pultruded composites, it is essential to obtain the force-displacement response and relationship with material conditions and collapse modes. Therefore, quasi-static compressive loading are conducted on pultruded composites.

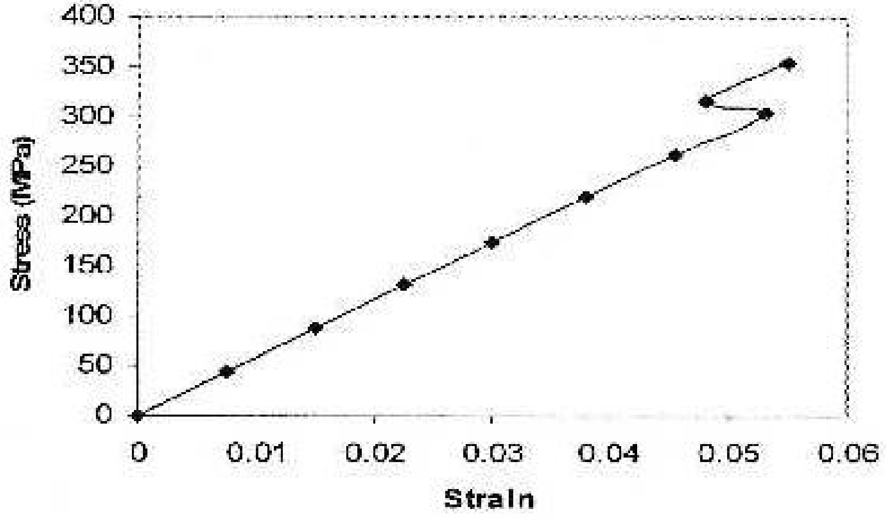

Figure 2: Stress versus strain of as-received pultruded composite

3.2.1 Square Pultruded Tubes with 3 mm Thickness

The forces-displacement responses of 3 mm thick composite chamfered with different angles are presented in Figure 3. Most of the material conditions reveal a typical curve for crashworthiness applications. Another important characteristic of these curves are the shape of the force-displacement curve. As the crushing begins, the load quickly rises to a peak value (elastic region) and then drops off significantly and stays relatively constant. Large force reduction occurred during the collapse showed that energy absorption performance decreased. For crashworthiness applications, the initial peak load, P_{peak} should not be much greater than the average or mean crush force, P_{mean} because large peak force required to initiate crushing and the goal in energy management is to absorb all the energy without imparting large forces to the people involved.

The load-displacement curves for 35° chamfering angle are shown in Figure 3(a). As can be seen here, higher peak load is sustained for the tubes crushed with smaller angles and there is a large amount of scatter of data especially at post-crushing region. The curves also exhibited an initial peak load followed by a large drop and then rise up to somewhat steady state. In the initial state of crushing, longitudinal cracks load increases, the fronts of the tube sides move outward and inward. Cracking process is observed along the tube corners as the compressive load increase. Then, the composites tubes failed catastrophically. Similar collapse mechanisms are also observed for other tubes chamfered with different angles and the force-displacement curves for each composite are shown in Figures 3(b) and 3(c).

The load-displacement for the tube chamfered with 45° angle is shown in Figure 3(b). The initial peak load for this type of angle is smaller than other composites. The composites are easily crushed and the wall tubes are slide out and collapse. The dominating failure mechanisms of the tube at the front end tip are shear compression failure which is micro-fragmented material at that tip has lowered the initial peak forces. After that, unstable crack propagation occurred along the tube corners and each wall side buckled catastrophically. This behavior result large reduction of peak force which is induced lower energy absorption performances.

The load-displacement of 55° chamfering angle at the front end tubes also reveled typical load-displacement curves as shown in Figure 3(c). Higher initial peak loads are obtained and the post-crushing regions are much smoother and insignificant force fluctuations are also observed. This is indicated that even though catastrophic collapse occurred for this type of chamfered end, the process of buckling mechanisms are observed to happen in stable manner.

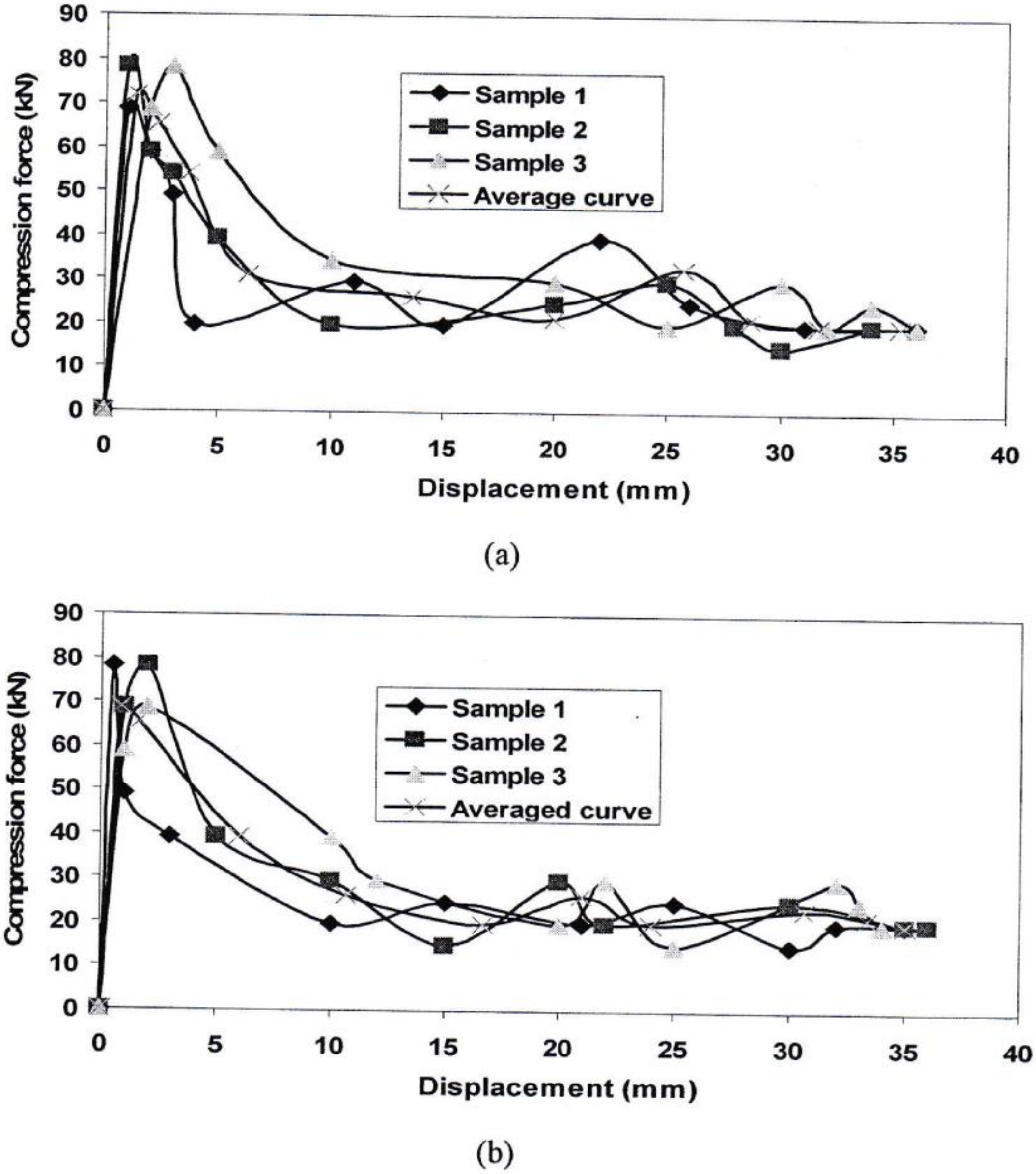

(a)

(b)

Figure 3: Force versus displacement response of pultruded composites 3 mm thickness, (a) 35°, (b) 45° and (c) 55° chamfering angles

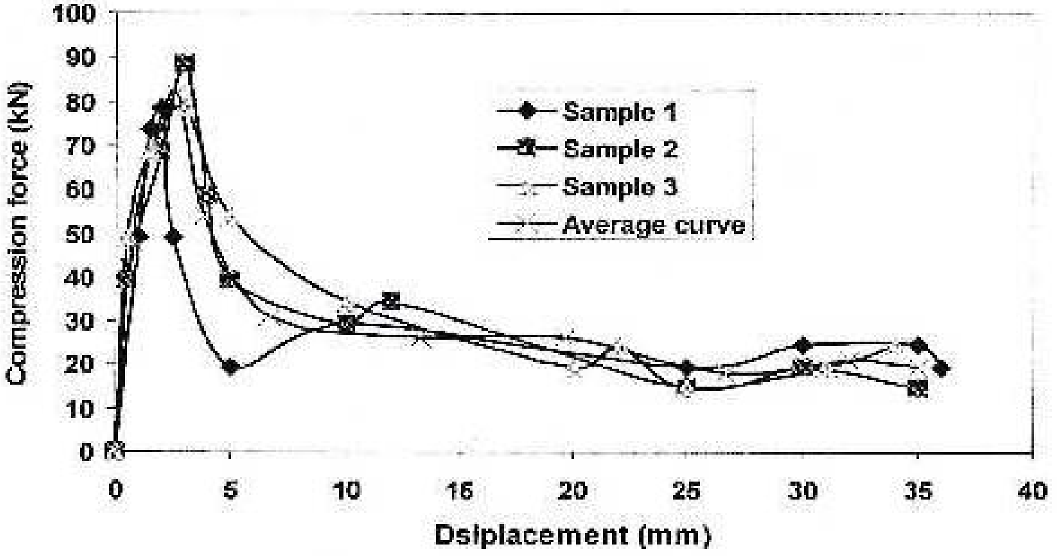

(c)

Figure 3: Force versus displacement response of pultruded composites 3 mm thickness, (a) 35°, (b) 45° and (c) 55° chamfering angles (continued)

3.2.2 Square Pultruded Tubes with 5 mm Thickness

Typical force versus displacement curves of pultruded composites are recorded and composite thickness has played an important role in modifying the curves and preventing sudden drop of peak forces as shown in Figure 4. The curves show the same trend when compared to other investigations [5-7, 10]. For 5 mm thick composites, the average load fluctuation almost constant after peak force up to final crushed deformation. The load-displacement traces rises sharply to a high peak as the composite undergoes elastic compression, this is then followed by progressive fracture collapse and crushing starts at chamfering angle at front end. Chamfering condition provides a critical zone for stress concentration and subsequently breaks the material within this region. Generally, chamfering is used to initiate the crushing process and prevent buckling failure mechanism that is minimized the energy absorption performance.

The force-displacement response of the tubes chamfered with 35° and 55° are almost similar in term of collapse modes as shown in Figures 4(a) and 4(c). Smooth post crushing regions are observed with little force striations. As the tubes are loaded, axial cracks form at the sides of the tubes spread away from the axial axis. Localized buckling occurred at the tube sides, this behavior created smooth force fluctuations. After reaching peak load, small drop of peak load is observed. The load then recovers to reach a steady state crushing process. Both tubes conditions show progressive collapse through localized buckling which are induced higher energy absorption capabilities. The force-displacement curves of collapse mode of 45° chamfered angle is shown in Figure 4(b). The initial peak force drops significantly due to 45° chamfering angle. This angle created a maximum shearing stress at around the front end tip. Fragmentation behavior of the material occurred around the tip especially at chamfered end. These fragmented materials are strengthened by fibers embedded in the matrix. This characteristic has caused large reduction or sudden drop occurred for 45° chamfered pultruded composite.

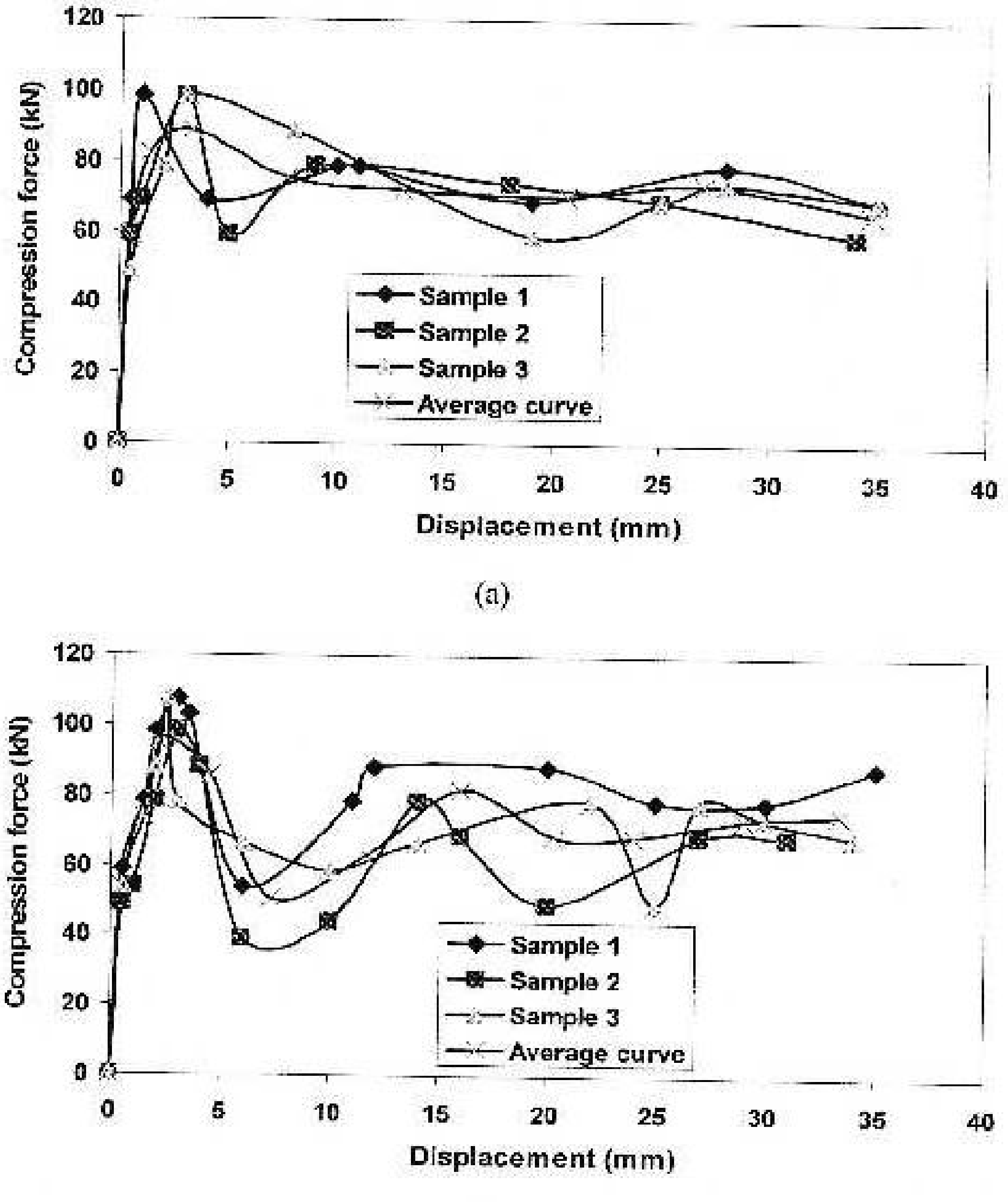

(a)

(b)

Figure 4: Force versus displacement response of pultruded composites 5 mm thickness, (a) 35°, (b) 45° and (c) 55° chamfering angles

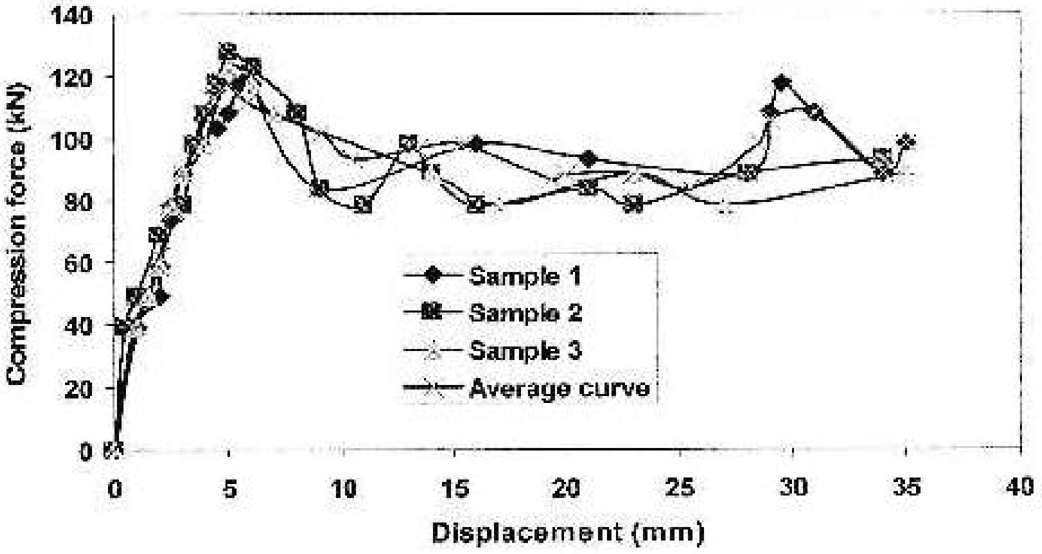

(c)

Figure 4: Force versus displacement response of pultruded composites 5 mm thickness, (a) 35°, (b) 45° and (c) 55° chamfering angles (continued)

3.2.3 Comparison Force-Displacement Responses

Previous investigation pertaining to the axial compression of thin-walled composites structures in the form of circular or square tubes and frusta [11-13] indicated that these composite shells deform in a manner different than similar structural components made of conventional materials. Plastic deformation is not the governing mechanisms but the extensive micro cracking development which may be easily controlled depending on the properties of the fibers and resins, as well as on the orientation of the fibers.

The force-displacement traces for the quasi-static compressions tests of square tubes of pultruded composites are shown in Figure 5. Obviously, typical force-displacement curves are observed and there are some differences occurred especially after initial deformation. As deformation progresses, the shape of these curves in Figure 5 depended significantly on chamfering angles and wall thickness. For 3 mm thick wall composites subjected to axial loading it is observed that the fracture behavior of the composite appear to affect the stability of the wall as well as magnitude of peak loads and the energy absorption during the crushing processes. Crack propagation instabilities are observed especially at wall corners. These crack propagation along these sides contributed to large peak load reduction due to catastrophic buckling failure mechanisms of the side walls as depicted in Figure 5(a).

Figure 5(b) shows slightly different mechanisms as observed in Figure 5(a). When load is applied axially to the chamfered edge of the tube, local failure of material occurred and small transverse cracks are formed in the region of chamfered edge. The lengths of these transverse cracks are dependent on crushing forces. The tip of the chamfered edge is bend inward of the tube. Linear deformation at the front edge tip is deformed in stable manner. After the curves reach the peak load, this load then experienced small load drop. Axial cracks are observed at the tube corners. The tube walls are bended progressively as deformation load increases. In the post-crushing region, small load fluctuations are observed as shown in Figure 5(a). In this investigation, the highest peak load is pertaining to 55° chamfered front end tubes and they are also induced the highest energy absorption capabilities.

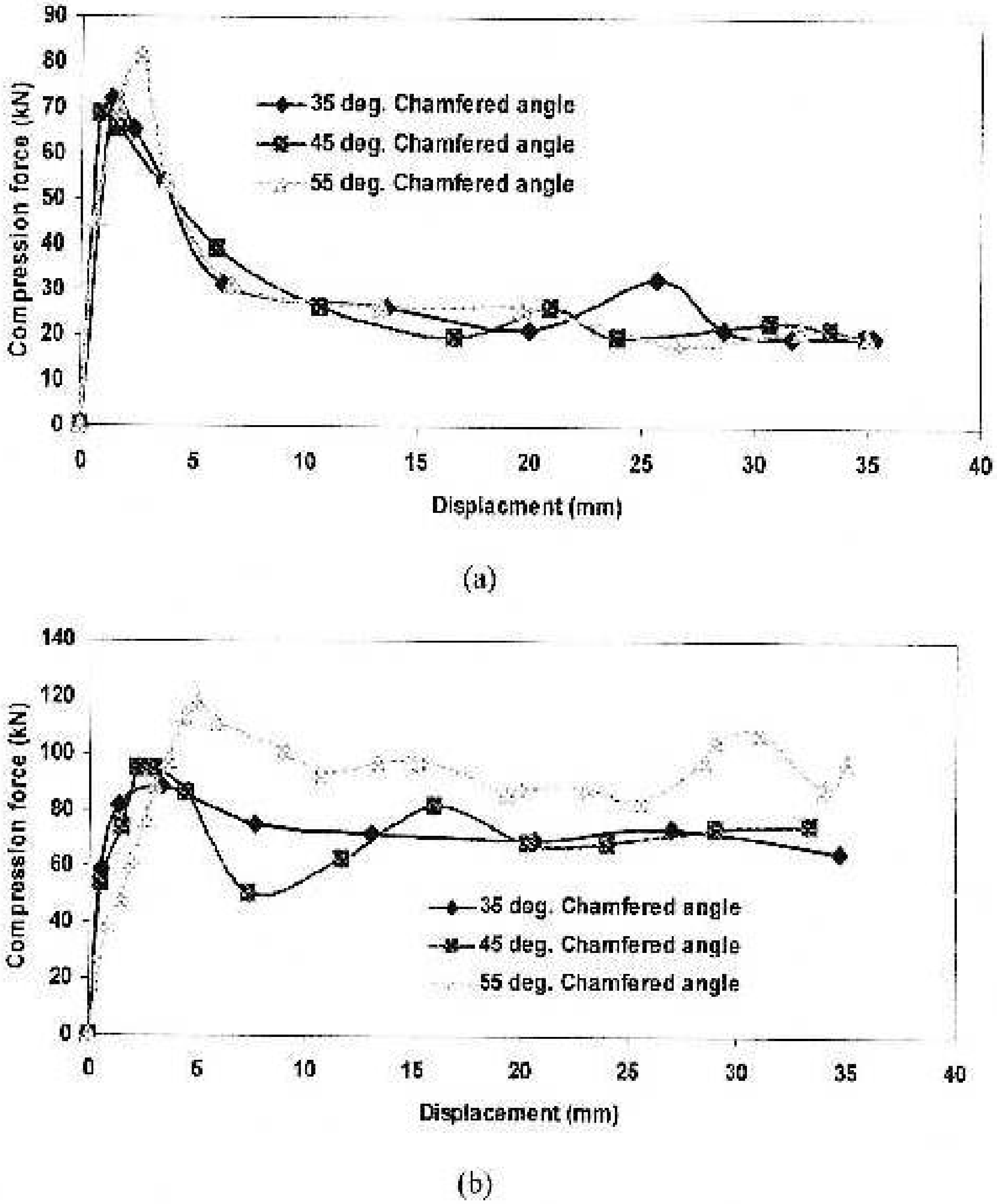

Figure 5: Comparisons of the force-displacement curves for pultruded composites with different wall thickness (a) 3 mm and (b) 5 mm

Taking into account the effect of chamfering angle at maximum shear compression failure mode occur at 45°. Crashworthiness behavior of this composite is greatly affected by this angle. It reduced the peak load and energy absorption performances. Micro-fragmentations occurred at the front edge tip without any side wall bending inward or outward of the tube. It other word, the material integrity at the front edge is crushed catastrophically.

3.3 Crashworthiness Parameters

3.3.1 Effect of Peak and Mean Forces

The peak and mean forces for quasi-statically crushed square tubes are shown in Figure 6. The dominant failure mechanisms for 3 mm and 5 mm composite wall thicknesses are buckling and progressive collapse modes, respectively leading to a high and low peak and mean forces. Composites tubes of 3 mm thick wall exhibited much more consistent behavior of both peak and mean force values, but insignificant energy absorption capability is recorded. 3 mm thick tube wall chamfered with 45° angle at the front end showed slightly lower peak and mean forces. Similar trend is also observed for 5 mm thick wall chamfered with 45° angle. Figure 6 also reveals that chamfering angles played an important role to vary the crashworthiness parameters. It is observed that increasing chamfering angles tend to increase peak and mean crushing forces.

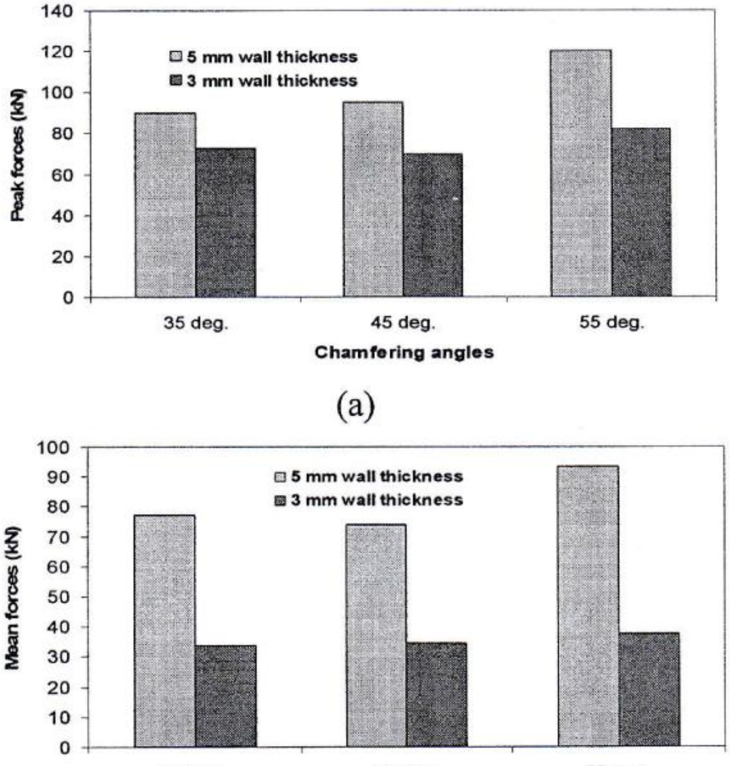

(a)

(b)

Figure 6: Chamfering angles effect on (a) peak force and (b) mean force on pultruded composites

3.3.2 *Effect of Load Ratio*

Figure 7 shows the effect of chamfering angle on load ratio. The load ratio clearly cannot be the only measure used to determine the crush efficiency and load ratio is independent on chamfering angles. The load ratio is defined as in Equation (2).

$$\text{Load ratio} = \frac{P_{Peak}}{P_{Mean}} \tag{2}$$

Equation (2) may be used for measuring crushing efficiency. Karbhari *et al.* [9] cited other sources that suggest the load ratio should be less than 1.25. Figure 7 also clearly shows that 3 mm thick wall composites have load ratios greater than load ratios for 5 mm thick wall composites. This ratio is closely related to collapse mechanisms that increasing or decreasing the energy absorption capabilities. Higher load ratio indicated that the composite tubes have buckled catastrophically. This sudden drop of initial peak load contributed to lower the area under force-displacement curves and therefore reducing the energy absorption performances. Global buckling is observed for 3 mm thick wall composites which one side of the tube walls has buckled in the middle of the tubes. 5 mm thick wall composites, stable axial cracking occurred along tube corners and followed with localized buckling where side wall of the composites moved inward and outward of the tubes leading to progressive collapses and then increased the energy absorption performances.

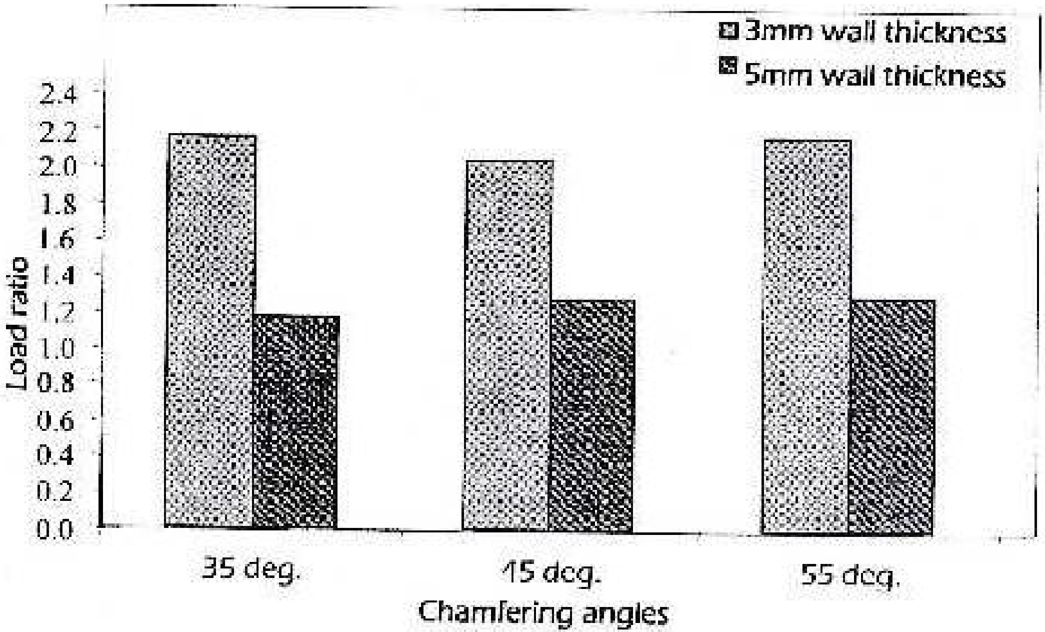

Figure 7: Effect of chamfering angle and wall thickness on load ratio of pultruded composites

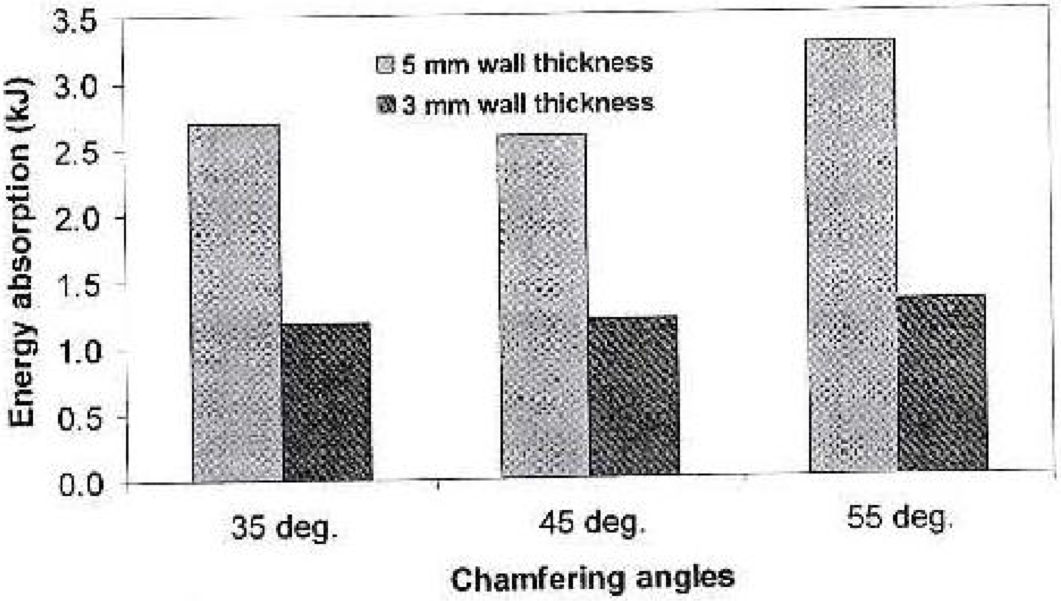

Figure 8: Effect of chamfering angles on energy absorption capabilities

3.3.3 Energy Absorption Capability

As-received composites that contained different front end chamfering angles are quasi-statically compressed under constant cross-head displacement are presented in Figure 8. Energy absorption performances are calculated by taking the average mean force multiplied by crushed deformation distance. Obviously, increasing composite wall thickness from 3 mm to 5 mm tends to increase the energy absorption capabilities almost double. For 3 mm thick wall composites, chamfering angles not played a crucial role in increasing the energy absorption performances while for 5 mm thick wall thickness composites increasing energy absorption capabilities are observed. This is related to the increasing crashworthiness parameters such peak and mean forces and composite geometries. Lower energy absorption performances are clearly observed for front end chamfered with 45° angle. Lower energy absorption capability is due to the fact that at this angle, the stress created at the chamfered end is a maximum shear compression. Therefore, the material around the chamfered tip is easily crushed into fragmented pieces of material.

3.4 Failure Modes

3.4.1 3 mm Thick Wall Pultruded Composites

An energy absorption performance of 3 mm thick wall pultruded composite was shown in Figure 8. Obviously, chamfering angles are independent on energy absorption capabilities. Micro fragmentation process is dominant failure mechanisms occurred especially in the front end region chamfered with 45° angle and induced lower energy absorption compared with other front end composite condition. Unstable axial cracks are observed along tube corners rather than progressive collapse. Unstable cracks created an individual side wall and as deformation progress, composite wall buckle catastrophically. Thus this reduces energy absorption performances. Figure 9 shows clearly the progression of buckling collapse of 3 mm thick wall pultruded composites. As deformation force increases, cracking process along tube corners firstly occurs as shown in Figure 9(b). The formation of these unstable crack propagations along tube corners resulted in reducing the energy absorption performances through catastrophic failure as shown in Figure 9(d).

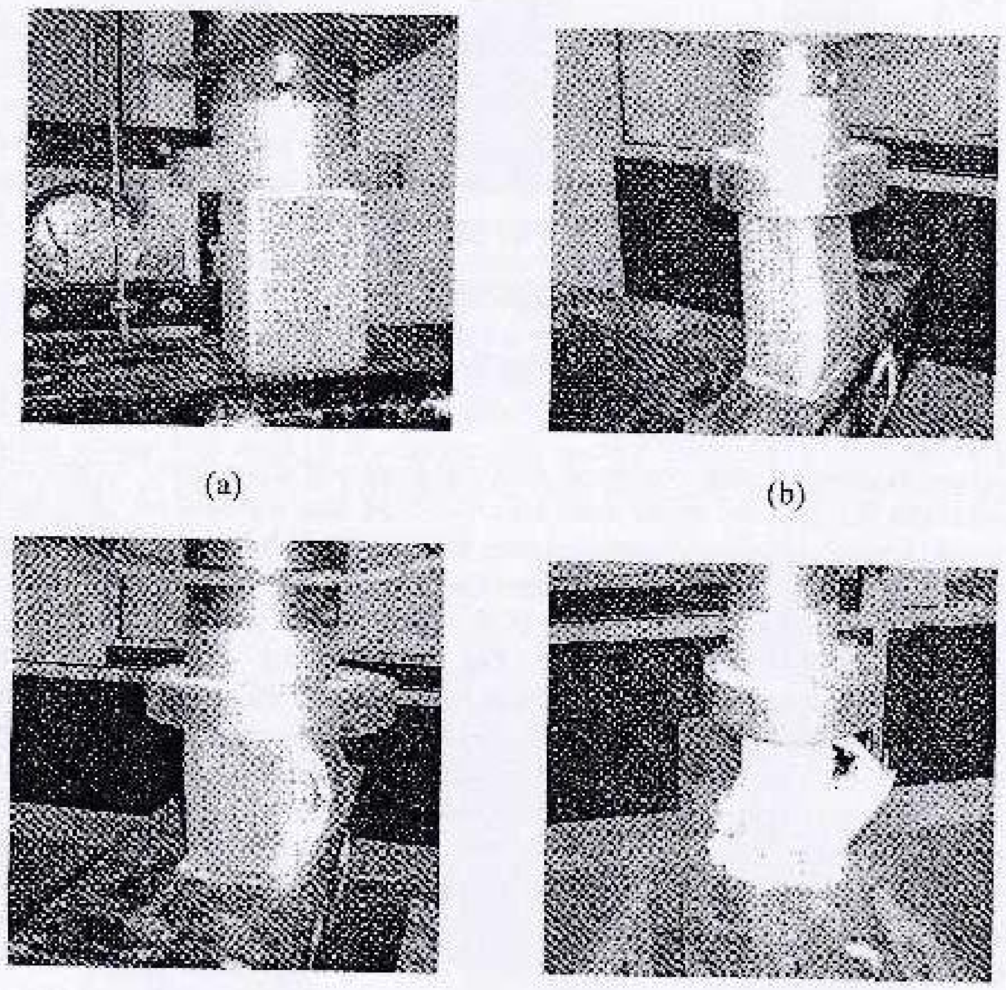

(a) (b)

(c) (d)

Figure 9: Collapse mechanisms of 3 mm thick wall pultruded composites

3.4.2 5 mm Thick Wall Pultruded Composites

Progressive collapses of the pultruded composites are observed to dominate failure mechanisms. This collapse failure starts at the top end of the structures and it is called mode-I progressive collapse. It is observed that the failure of the composites remains intact without material fragmentation and thereby this composite exhibits post-crushing integrity strength. As the crushing progresses, the stresses at chamfered end increased and the concentrated stresses exceed the matrix strength and matrix cracking occurs. The mode-I of failure similar to a "mushrooming" failure [6] is characterized by progressive collapse through the formation of continuous fronds which spread outwards and inwards, see Figure 10. This figure shows the sequence of progressive collapse mode of pultruded composite contained 55° of chamfering angle. As deformation precedes further, the externally formed fronds curl downwards with the simultaneous development of four axial split followed by splaying of the material strips. According to Figure 10.0 of pultruded composite chamfered with 55° angle. This chamfering angle induced the highest energy absorption performance. Progressive collapse mechanisms through localized wall buckling created higher energy absorption capability.

Figures 10(b) and 10(c) reveal the localized wall buckling after axial cracking along tuber corners in stable manner. Then, the subsequent collapse mechanism is shown in Figures 10(d) and 10(e). Fronds of the tube walls are bended inward and outward. Matrix dominated failure behaviors are seen throughout the progressive collapse. Similar collapse mechanisms are recorded for other pultruded composites chamfered with 35° and 45°.

4.0 CONCLUSION

Quasi-static experimental investigations on the crashworthiness behaviors of pultruded composites have been carried out under compressive loading. The conclusions of the works are summarized as follow:

- Both mean and peak forces are greatly affected by chamfering angles for 5 mm thick wall pultruded composites but 3 mm thick wall composites, these angles not played an important role.
- Higher energy absorption capabilities are recorded for 5 mm thick wall composites rather than 3 mm thick wall composites. The difference of energy absorptions of these both tube thicknesses are almost double which energy absorption for 5 mm thick wall is higher than 3 mm thick wall. But the energy absorption capability for 3 mm thick wall is not depend on the chamfering angles.
- Peak force for tubes chamfered with 45° angle is the lowest due to micro-fragmentation occurred in the region of front end.
- For the most cases, crashworthiness parameters and behavior for tubes chamfered with 55° is better than other tube conditions.
- For 5 mm thick wall pultruded composites, progressive collapse mechanisms are observed through localized wall buckling after axial cracking along tube corners, while for 3 mm thick wall composites, unstable crack propagation occurred along tube corners and created global wall buckling.
- Different collapse mechanisms induced different crashworthiness behavior.

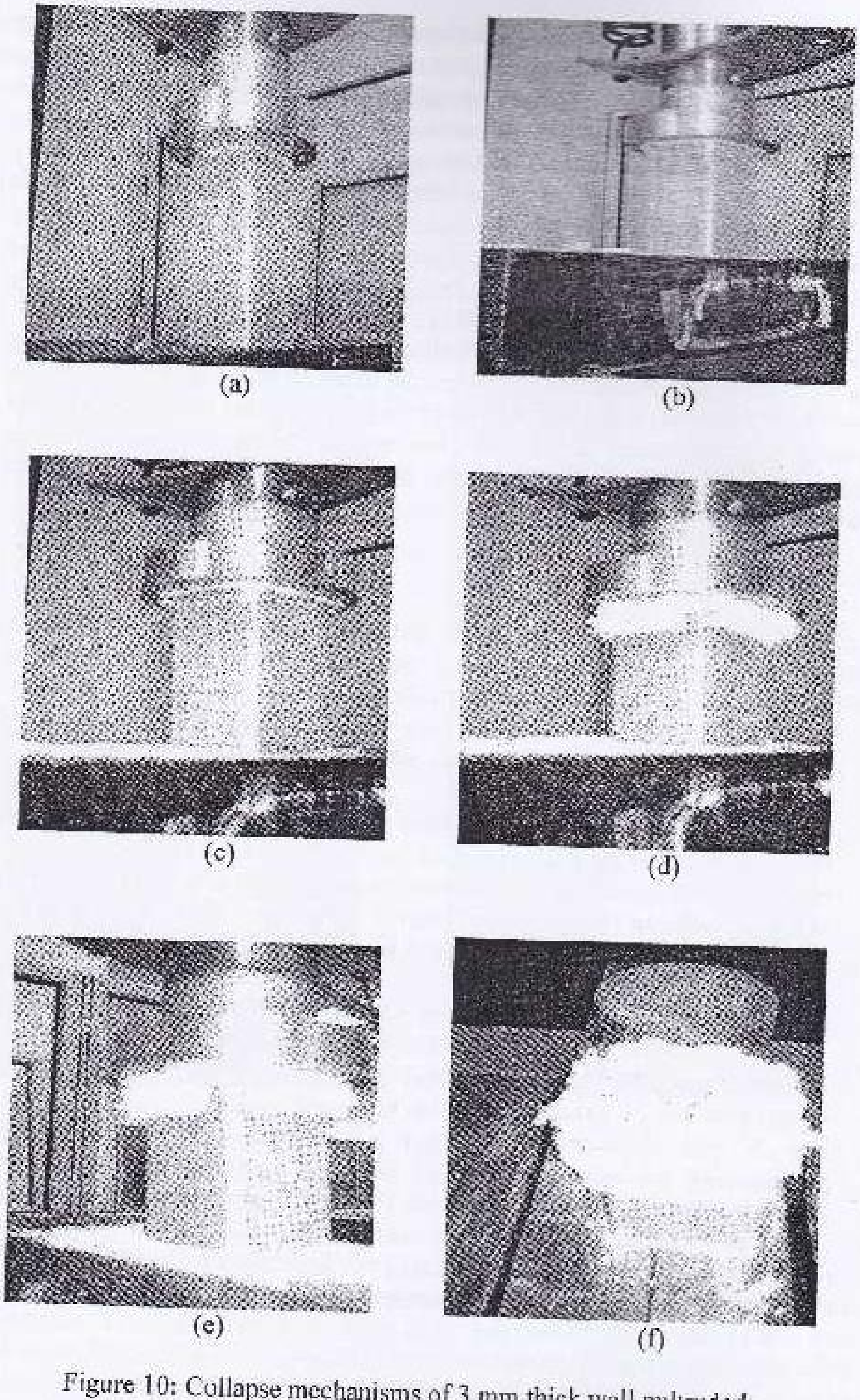

(a) (b)

(c) (d)

(e) (f)

Figure 10: Collapse mechanisms of 3 mm thick wall pultruded composites for 55° chamfered angle

REFERENCES

1. Hamada, H., Kameo, K., Sakaguchi, M., Saito, H., Iwamoto, M., 2000. *Energy absorption properties of braided composite rods,* Composites Science & Technology, 60, 723-729.
2. Wallentowitz, H., Adam, H., 1995. The use of energy absorbing reinforcements in automotive applications, *SAMPE Journal,* 31(5), 23-28.
3. Thornton, P.H., 1979. Energy absorption in composite structures, *Journal of Composite Materials,* 13, 247-263.
4. Thornton, P.H., 1990. *The crush of fiber reinforced plastics, in Handbook of ceramics and composites,* Vol. 1: Synthesis and properties, Cheremisin off, N.P. ed. Marcel Dekker Inc., New York, 307-337.
5. Hull, D., 1982. *Energy absorption of composite materials under crash conditions,* Proceedings of the 4th International Conference on Composite Materials, 1, 307-337.
6. Farley, G.L., Jones, R.M., 1992. Crushing characteristics of composite tubes with near-elliptical cross section, *Journal of Composite Materials*, 26(12), 1741-1751.
7. Farley, G.L., Jones, R.M., 1991. The effect of crushing speed on the energy absorption capability of composite tubes, *Journal of Composite Materials*, 25, 1314-1329.
8. Saiphon, C., Lawrence, Bank, C., Michael, Plesha, E., 2004. *Progressive tearing failure in pultruded composite material tubes,* Composite Structures, 63(1), 45-52.
9. Karbhari, V.M., Fazlon, M., Paul, J., Herzberg, I., 1997. Energy absorption characteristics of hybrid braided composite tubes, *Journal of Composite Materials,* 31(12), 1165-1186.
10. Asad, A.K., Sahari, B.B., Khalid, Y.A., 2002. *Performance of composite cones under axial compression loading,* Composites Science & Technology, 62, 17-27.
11. Mamalis, A.G., Manolakos, D.E., Demosthenous, G.A., Ioannidis, M.B., 1997. *The static and dynamic axial crushing crumbling of thin walled fiber glass composite square tubes,* Composites 28B, 439-451.
12. Mamalis, A.G., Manolakos, D.E., Demosthenous, G.A., Ioannidis, M.B., 1994. *Analysis of failure mechanisms observed in axial collapse of thin-walled circular fiber glass composite tubes,* Thin-Walled Structures, 26, 436-444.
13. Mamalis, A.G., Manolakos, D.E., Vigelahn, G.L., Yap, S.M., Demosthenous, G.A., 1991. Microscopic failure of thin-walled fiber reinforced composite frusta under static axial collapse, *International Journal of Vehicle Design*, 12, 557-563.